8594 *Biochemistry* **2009,** *48,* 8594–8602
DOI: 10.1021/bi901127s

BIOCHEMISTRY
including biophysical chemistry & molecular biology
Article

Probing the Allosteric Modulator Binding Site of GluR2 with Thiazide Derivatives[†]

Christopher P. Ptak,[§] Ahmed H. Ahmed,[§] and Robert E. Oswald*

Department of Molecular Medicine, Cornell University, Ithaca, New York 14853 [§]*These authors contributed equally to this work.*

Received July 2, 2009; Revised Manuscript Received August 11, 2009

ABSTRACT: Ionotropic glutamate receptors mediate the majority of vertebrate excitatory synaptic transmission and are therapeutic targets for cognitive enhancement and treatment of schizophrenia. The binding domains of these tetrameric receptors consist of two dimers, and the dissociation of the dimer interface of the ligand-binding domain leads to desensitization in the continued presence of agonist. Positive allosteric modulators act by strengthening the dimer interface and reducing the level of desensitization, thereby increasing steady-state activation. Removing the desensitized state for simplified analysis of receptor activation is commonly achieved using cyclothiazide (CTZ), the most potent modulator of the benzothiadiazide class, with the flip form of the AMPA receptor subtype. IDRA-21, the first benzothiadiazide to have an effect in behavioral tests, is an important lead compound in clinical trials for cognitive enhancement as it can cross the blood−brain barrier. Intermediate structures between CTZ and IDRA-21 show reduced potency, suggesting that these two compounds have different contact points associated with binding. To understand how benzothiadiazides bind to the pocket bridging the dimer interface, we generated a series of crystal structures of the GluR2 ligand-binding domain complexed with benzothiadiazide derivatives (IDRA-21, hydroflumethiazide, hydrochlorothiazide, chlorothiazide, trichlormethiazide, and althiazide) for comparison with an existing structure for cyclothiazide. The structures detail how changes in the substituents at the 3- and 7-positions of the hydrobenzothiadiazide ring shift the orientation of the drug in the binding site and, in some cases, change the stoichiometry of binding. All derivatives maintain a hydrogen bond with the Ser754 hydroxyl, affirming the partial selectivity of the benzothiadiazides for the flip form of AMPA receptors.

Ionotropic glutamate receptors (iGluRs) are the major mediators of excitatory synaptic transmission in the vertebrate central nervous system (*1*) and play important roles in processes such as learning and memory as well as in neuronal development (*2*). In addition, iGluRs have been implicated in various neurodegenerative disorders such as Parkinson's and Alzheimer's diseases, Huntington's chorea, and neurologic disorders, including epilepsy and ischemic brain damage. iGluRs are a class of ligand-gated ion channels composed of four membrane-bound subunits. Each subunit contains a ligand-binding domain tethered to pore-forming helices, which surround a central ion conduction pathway (*3*−*5*). The ligand-binding domain is composed of two lobes that close upon agonist binding (*6*). Activation (i.e., channel opening) is a conformationally coupled response to agonist-induced lobe closure. Through different pathways, deactivation and desensitization return iGluRs to a closed state. In the presence of agonist, desensitization is an important physiological mechanism that prevents excess current from entering the cell. Controlling the rate at which iGluRs enter the desensitized state is pharmacologically important for prolonging the excitatory effects of activation.

AMPA[1] receptors (GluR1−4), a subtype of the iGluR family, are categorized by sensitivity to the synthetic agonist α-amino-3-hydroxy-5-methyl-4-isoxazolepropionic acid (AMPA). The AMPA receptors exist in two splice variants (flip and flop) that differ in their rates of desensitization (*7*) and channel closing (*8*). Allosteric modulators of AMPA receptors are known to block desensitization, slow deactivation, and enhance synaptic plasticity. These characteristics have led to clinical trials of several drugs for Alzheimer's disease and attention deficit disorder (*9*, *10*), but only aniracetam is available for mild dementia in Europe (*11*). The benzothiadiazide class of diuretics can also act as positive allosteric modulators of AMPA receptors, with the most potent being cyclothiazide (*12*, *13*). In most cases, these drugs do not pass the blood−brain barrier and do not have central effects on AMPA receptors in vivo. A saturated diazoxide derivative, IDRA-21, was found to pass the blood−brain barrier

[†]This work was supported by grants from the National Institutes of Health (R01-GM068935) and is based in part upon research conducted at the Cornell High Energy Synchrotron Source (CHESS), which is supported by the National Science Foundation by Grant DMR 0225180, using the Macromolecular Diffraction at the CHESS (MacCHESS) facility, which is supported by Grant RR-01646 from the National Institutes of Health, through its National Center for Research Resources. C.P.P. was supported in part by NIH Training Grant T32CA09682.

*To whom correspondence should be addressed. Telephone: (607) 253-3877. Fax: (607) 253-3659. E-mail: reo1@cornell.edu.

[1]Abbreviations: ALTZ, althiazide; AMPA, α-amino-3-hydroxy-5-methyl-4-isoxazolepropionic acid; CLTZ, chlorothiazide; CX614, pyrrolidino-1,3-oxazinobenzo-1,4-dioxan-10-one; CTZ, cyclothiazide; FW, (*S*)-5-fluorowillardiine; flip and flop, alternatively spliced versions of AMPA receptors that vary in their rates of desensitization and sensitivity to allosteric modulators; GluR, ionotropic glutamate receptor; HCTZ, hydrochlorothiazide; HFMZ, hydroflumethiazide; IDRA-21, 7-chloro-3-methyl-3,4-dihydro-2*H*-benzo[*e*][1,2,4]thiadiazine 1,1-dioxide; IPTG, isopropyl *β*-D-thiogalactoside; PEPA, 4-[2-(phenylsulfonylamino)ethylthio]-2,6-difluorophenoxyacetamide; NMDA, *N*-methyl-D-aspartic acid; rmsd, root-mean-square deviation; S1S2, extracellular ligand-binding domain of GluR2; SARs, structure−activity relationships; TCMZ, trichlormethiazide.

 Published on Web 08/12/2009

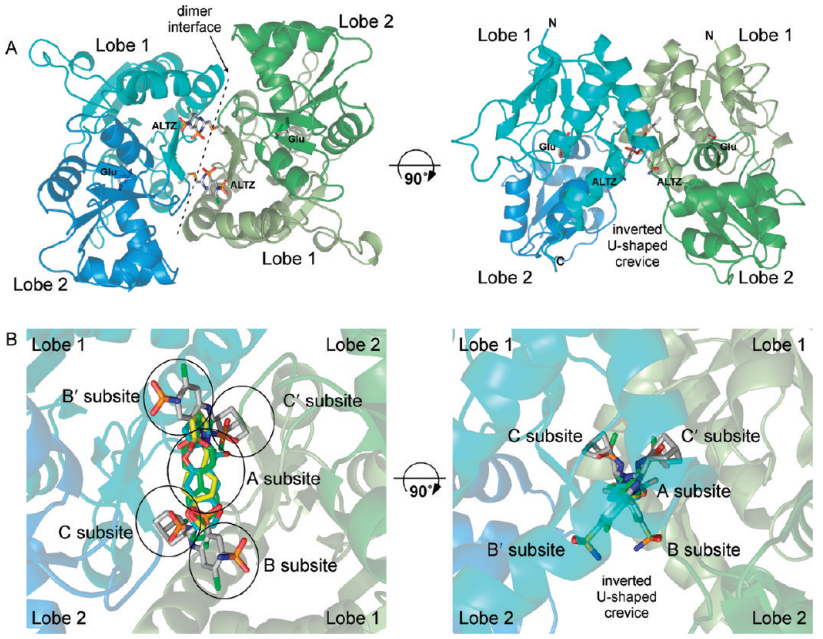

FIGURE 1: (A) Structure of the GluR2 S1S2 dimer in two orientations. One monomer is shown in shades of blue and the other in shades of green. ALTZ is bound in two copies to the dimer interface, and glutamate is bound to the agonist-binding site. The structures on the left illustrate the symmetrical dimer interface, and the structures on the right illustrate the inverted U-shaped cleft between the subunits. (B) Illustration of the five subsites in the binding surface by superimposition of structures determined previously. The ribbon representation of the protein is from the cyclothiazide structure [PDB entry 1lbc (*18*)]. The carbon atoms in CTZ are colored white. Also shown are the positions for aniracetam [PDB entry 2al5; carbons colored yellow (*20*)], CX614 [PDB entry 2al4; carbons colored cyan (*20*)], and a dimeric biarylpropylsulfonamide [PDB entry 3bbr, carbons colored green (*21*)]. In the cases of aniracetam and CX614, only one of two orientations is shown.

and was found to have positive effects on cognition (*14*−*16*). The benzothiadiazide-derived allosteric modulators are being utilized as lead compounds in extensive SAR studies with the potential to increase specificity and potency in vivo.

At the molecular level, allosteric modulators target the desensitization process by stabilizing the activated-state quaternary assembly of ligand-binding domains. The ligand-binding domain of AMPA receptors is assembled into a dimer of dimers relative to the more symmetrical assembly of the tetrameric channel-forming domain. AMPA receptor desensitization is largely removed in the L483Y mutant, effectively increasing the steady-state current response (*17*). L483Y stabilizes ligand-binding domain dimers by burying into the neighboring helix across the dimer interface at two identical sites (*18*). In a similar way, allosteric modulators act on the dimer interface of the GluR2 ligand-binding domain, which forms an inverted U-shaped crevice with 2-fold symmetry (Figure 1A). The first structure of an allosteric modulator bound to the isolated binding domain of the GluR2 AMPA subunit structure was that of cyclothiazide (CTZ) (*18*). The drug binds in two copies to the dimer interface, which forms a stable bridge across the dimer interface and inhibits desensitization. CTZ is moderately selective for the flip isoform of AMPA receptors and makes a hydrogen bond through the 4-nitrogen to S754 (which is an asparagine in the flop isoform) (*19*). Structures of several other allosteric modulators with the GluR2 dimer have been determined [aniracetam (*20*), CX614 (*20*), a dimeric biarylpropylsulfonamide (*21*), and several CTZ derivatives (*22*)].

The large symmetrical surface at the dimer interface can be dissected into an association of five overlapping subsites (Figure 1B). The central subsite (A subsite) and two symmetrical copies of two subsites (B and C subsites) are bordered by residues from each of the two monomers. An overlay of the crystal structures of four allosteric modulators reveals how the full interface can be occupied. Individual modulators occupy different combinations of subsites and therefore impose stable linkages between different structural elements of the ligand-binding domain dimer. Aniracetam and CX614 both fully occupy central subsite A but do not bind to either the B or C subsite. CTZ can be considered to be part of a separate class of allosteric modulators that occupy both the B and C subsites and only part of the A subsite. The symmetry of the B and C subsites allows two CTZ molecules to bind to the dimer interface and fill the more peripheral borders of the crevice. The fourth modulator structure, a synthetic dimeric biarylpropylsulfonamide, illustrates how a compound could be designed to bridge the two CTZ binding sites extending from the C subsite to the C′ subsite.

Although allosteric modulators generally prolong steady-state current, the details of receptor regulation in terms of regulation of binding, changes in deactivation, and sensitivity to mutation suggest that functional differences may be related to subsite binding patterns. In addition to slowing desensitization, CX614 increases the level of equilibrium agonist binding (*23*), while conversely CTZ decreases the level of equilibrium agonist binding (*24*). Being of the same class of benzothiadiazides as CTZ, an IDRA-21 derivative, D1, surprisingly increases the level of equilibrium agonist binding (*25*). These effects may be due to changes in conformational equilibria induced by the modulators or changes in the agonist-binding site. An additional distinction has been made between IDRA-21 and CTZ. Substitutions at several positions on the parent, benzothiadiazide, have almost opposite effects for IDRA-21 and CTZ (*26*, *27*). For example, at the 5-position, a substitution in IDRA-21 greatly enhances activity while in CTZ results in a loss of activity. To explain the disparate results within the benzothiadiazide class, binding contacts and possibly even the binding pocket of IDRA-21 and CTZ have been suggested to be distinct (*26*, *27*). To explain how the structurally similar class of benzothiadiazides could have

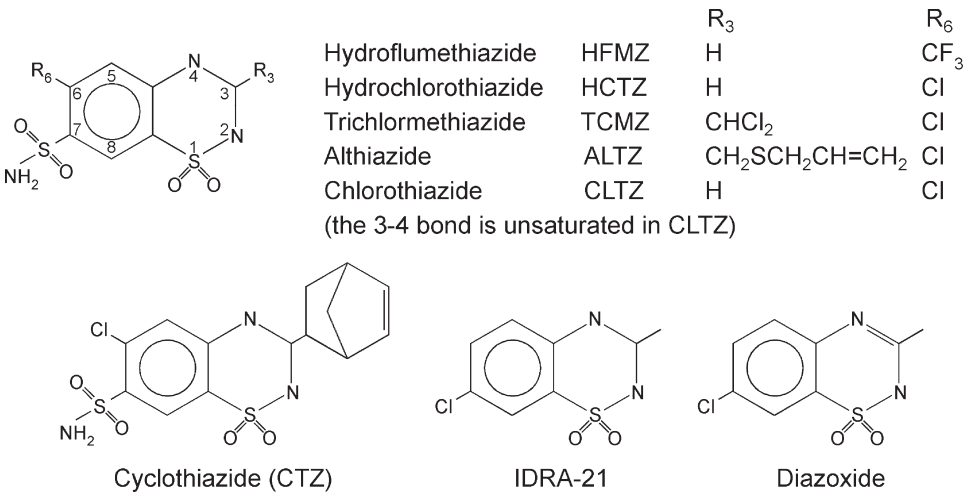

FIGURE 2: Structures of the allosteric modulators.

divergent effects on AMPA receptors, we have determined the structures of six thiazide derivatives (Figure 2; the structure bound to diazoxide was also determined, but the density for diazoxide was weaker than for the other compounds) bound to the GluR2 dimer interface. All six compounds form a similar hydrogen bond to S754, but the orientations within the site vary significantly, with differential occupations of the subsites. Both the orientation in the binding site (and thus the occupation of the subsites) and the stoichiometry are affected largely by modifications of the thiazide ring in the 3-position. Differences in the structures begin to explain a number of factors that contribute to the occupation of the five subsites.

EXPERIMENTAL PROCEDURES

Materials. IDRA-21 and diazoxide were purchased from Tocris (Ellisville, MO), and fluorowillardiine (FW) was purchased from Ascent Scientific (Princeton, NJ). ALTZ, CLTZ, HCTZ, HFMZ, and TCMZ were purchased from Sigma-Aldrich (St. Louis, MO). The GluR2 S1S2J construct was obtained from E. Gouaux (Vollum Institute) (*6*).

Protein Preparation and Purification. S1S2 consists of residues N392−K506 and P632−S775 of the full rat GluR2 flop subunit (*28*) with the N754S mutation, a "GA" segment at the N-terminus, and a "GT" linker connecting K506 and P632 (*6*). pET-22b(+) plasmids were transformed in *Escherichia coli* strain Origami B(DE3) cells and were grown at 37 °C to an OD_{600} of 0.9−1.0 in LB medium supplemented with antibiotics (ampicillin and kanamycin). The cultures were cooled to 20 °C for 20 min, and isopropyl β-D-thiogalactoside (IPTG) was added to a final concentration of 0.5 mM. Cultures were allowed to grow at 20 °C for 20 h. The cells were then pelleted, and the S1S2 protein was purified using a Ni-NTA column, followed by thrombin cleavage of the six-His tag, a sizing column (Superose 12, XK 26/100), and finally an HT-SP ion exchange Sepharose column (Amersham Pharmacia). Glutamate (1 mM) was maintained in all buffers throughout the purification. After the last column, the protein was concentrated and stored in 20 mM sodium acetate, 1 mM sodium azide, and 10 mM glutamate (pH 5.5). For ^{19}F NMR studies, FW was exchanged into the sample by successive concentration [Amicon Ultra-4 (10K) filter] and dilution using buffer only in the first few steps followed by 5 mM ligand.

Crystallography. For crystallization trials, the protein was concentrated to 0.3−0.4 mM in 10 mM glutamate using a Centricon 10 centrifugal filter (Millipore, Bedford, MA), and the six thiazide derivatives were dissolved in DMSO and added to a final concentration of 3 mM. The final protein concentration was approximately 0.3 mM. Crystals were grown at 4 °C using the hanging drop technique, and the drops contained a 1:1 (v/v) ratio of protein solution to reservoir solution. The reservoir solution contained 16−18% PEG 8K, 0.1 M sodium cacodylate, and 0.1−0.15 M zinc acetate (pH 6.5).

Data were collected at Cornell High Energy Synchrotron Source beamline A1 using a Quantum-210 Area Detector Systems charge-coupled device detector. Data sets were indexed and scaled with HKL-2000 (*29*). Structures were determined with molecular replacement using Phenix (*30*). Refinement was performed with Phenix (*30*), and Coot 0.5 (*31*) was used for model building. The starting models for the allosteric modulators were generated in JMEMolecularEditor (Novartis AG) and refined in Phenix (*30*).

NMR Spectroscopy. ^{19}F NMR spectra were recorded using a broadband probe on a Varian Inova 500 spectrometer with the proton channel downtuned to fluorine (470 MHz). Spectra were processed using NMRPipe version 1.6 (*32*). Linear prediction was used to reconstruct the first 14 points of the free induction decay, and the data were apodized with a mixed exponential-Gauss window function and zero-filled to double the original number of data points before Fourier transformation.

RESULTS

Structure Determination. The structure of glutamate bound to GluR2 S1S2 [PDB entry 3dp6 (*33*)] was used as the initial search probe for the molecular replacement solution [Phenix (*30*)] of six thiazide derivatives (Figure 2) bound to GluR2 S1S2 with glutamate in the agonist-binding site. In each case, additional density was observed at the dimer interface between two S1S2 monomers that corresponded to the thiazide binding sites. The thiazide derivatives were modeled into the density using Coot (*31*) and refined further with Phenix (*30*). The refinement statistics are listed in Table 1. In each case, three unique copies were found per unit cell, and the resolution ranged from 2.0 to 2.9 Å.

ALTZ and TCMZ. The structure of GluR2 S1S2 bound to cyclothiazide has been determined previously [PDB entry 1lbc (*18*)]. The hydrobenzothiadiazide rings of TCMZ and ALTZ overlay the position of cyclothiazide, with the sulfonamide group

Table 1: Structural Statistics

	TCMZ	ALTZ	HCTZ
space group	$P22_12_1$	$P22_12_1$	$P22_12_1$
unit cell (Å)	a = 45.2, b = 107.8, c = 157.9	a = 47.6, b = 114.6, c = 164.6	a = 47.4, b = 114.4, c = 162.9
X-ray source	CHESS (A1)	CHESS (A1)	CHESS (A1)
wavelength (Å)	0.977	0.977	0.977
resolution (Å)	50−2.2 (2.24−2.20)	50−2.0 (2.03−2.00)	50.0−2.9 (2.95−2.90)
no. of measured reflections	218384	404537	142366
no. of unique reflections	43133	61344	20653
data redundancy	5.1 (5.1)	6.6 (5.2)	6.9 (6.0)
completeness (%)	99.9 (100.0)	99.8 (99.5)	99.9 (99.5)
R_{sym} (%)	11.0 (61.8)	15.9 (69.8)	17.9 (80.6)
I/σ_I	19.3 (2.2)	21.7 (2.4)	16.5 (2.5)
PDB entry	3ILT	3IJO	3IJX
	Current Model Refinement Statistics		
phasing	MR	MR	MR
no. of molecules per asymmetric unit	3	3	3
R_{work}/R_{free} (%)	21.0/26.1	19.6/23.4	18.6/25.8
free R test set size [no. (%)]	2000 (5.4)	1995 (3.6)	1922 (10.0)
no. of protein atoms	6054	6054	6054
no. of heteroatoms	60	66	51
rmsd for bond lengths (Å)	0.012	0.007	0.009
rmsd for bond angles (deg)	1.47	1.09	1.16

	HFMZ	CLTZ	IDRA-21
space group	$P22_12_1$	$P22_12_1$	$P22_12_1$
unit cell (Å)	a = 47.3, b = 114.2, c = 163.7	a = 47.5, b = 114.1, c = 163.4	a = 47.3, b = 114.7, c = 165.4
X-ray source	CHESS (A1)	CHESS (A1)	CHESS (A1)
wavelength (Å)	0.977	0.977	0.977
resolution (Å)	50−2.0 (2.03−2.00)	50−2.1 (2.14−2.1)	50.0−2.0 (2.03−2.00)
no. of measured reflections	431453	368186	379519
no. of unique reflections	60617	52365	60130
data redundancy	7.1 (6.1)	7.0 (5.6)	6.3 (4.9)
completeness (%)	99.9 (99.9)	99.0 (96.2)	97.5 (86.6)
R_{sym} (%)	14.5 (78.1)	12.3 (71.6)	9.6 (67.7)
I/σ_I	18.3 (2.3)	22.1 (2.1)	27.0 (2.4)
PDB entry	3ILU	3IK6	3IL1
	Current Model Refinement Statistics		
phasing	MR	MR	MR
no. of molecules per asymmetric unit	3	3	3
R_{work}/R_{free} (%)	18.8/22.6	19.7/24.5	18.7/23.4
free R test set size [no. (%)]	2000 (3.6)	1997 (4.2)	2000 (3.5)
no. of protein atoms	6054	6054	6054
no. of heteroatoms	60	51	42
rmsd for bond lengths (Å)	0.009	0.006	0.007
rmsd for bond angles (deg)	1.19	0.973	1.05

in a hydrophilic pocket consisting of the side chain of K763, the backbone amide of S497, the side chain hydroxyl of Y424, the backbone carbonyl of F495, and the side chain hydroxyl of S729 [pocket B (Figure 3A)]. The water molecule mediating the hydrogen bond network among K763, the backbone carbonyl of S497, and the sulfonamide oxygen that is present in the CTZ structure is also found in the ALTZ structure but not the TCMZ structure. The sulfone interacts with the side chain of S497 and through a water molecule with the carbonyl of K730. The norbornenyl group of CTZ, the dichloromethyl group of TCMZ, and the (2-propenylthio)methyl group of ALTZ inserts into the hydrophobic pocket [pocket C (Figure 3A)] lined with I481, the methylene groups of the side chain of K493, and L751. Perhaps the most important interaction is that of the 4-nitrogen with S754, which is the basis of the moderate selectivity of this class of compounds for the flip form of AMPA receptors. The flop form has an asparagine in this position, which destabilizes binding of the thiazides.

HFMZ, HCTZ, and CLTZ. Removal of the hydrophobic group in the 3-position, as seen in HFMZ, HCTZ, and CLTZ, results in a rotation of the hydrobenzothiadiazide ring in the binding site, while the hydrogen bond with the side chain hydroxyl of S754 is maintained. This leaves the hydrobenzothiadiazide ring in approximately the same plane, but the ring moves into the hydrophobic pocket occupied by the norborenyl group of CTZ [C subsite (Figure 3B)]. This would suggest that the hydrophobic interactions in the C subsite are essential to the binding affinity and are occupied preferentially. This rotation of the hydrobenzothiadiazide ring in HFMZ, HCTZ, and CLTZ leaves a space (B subsite) that is filled by six additional water molecules. This would be energetically favored because the C subsite is more hydrophobic and is deeper in the U-shaped

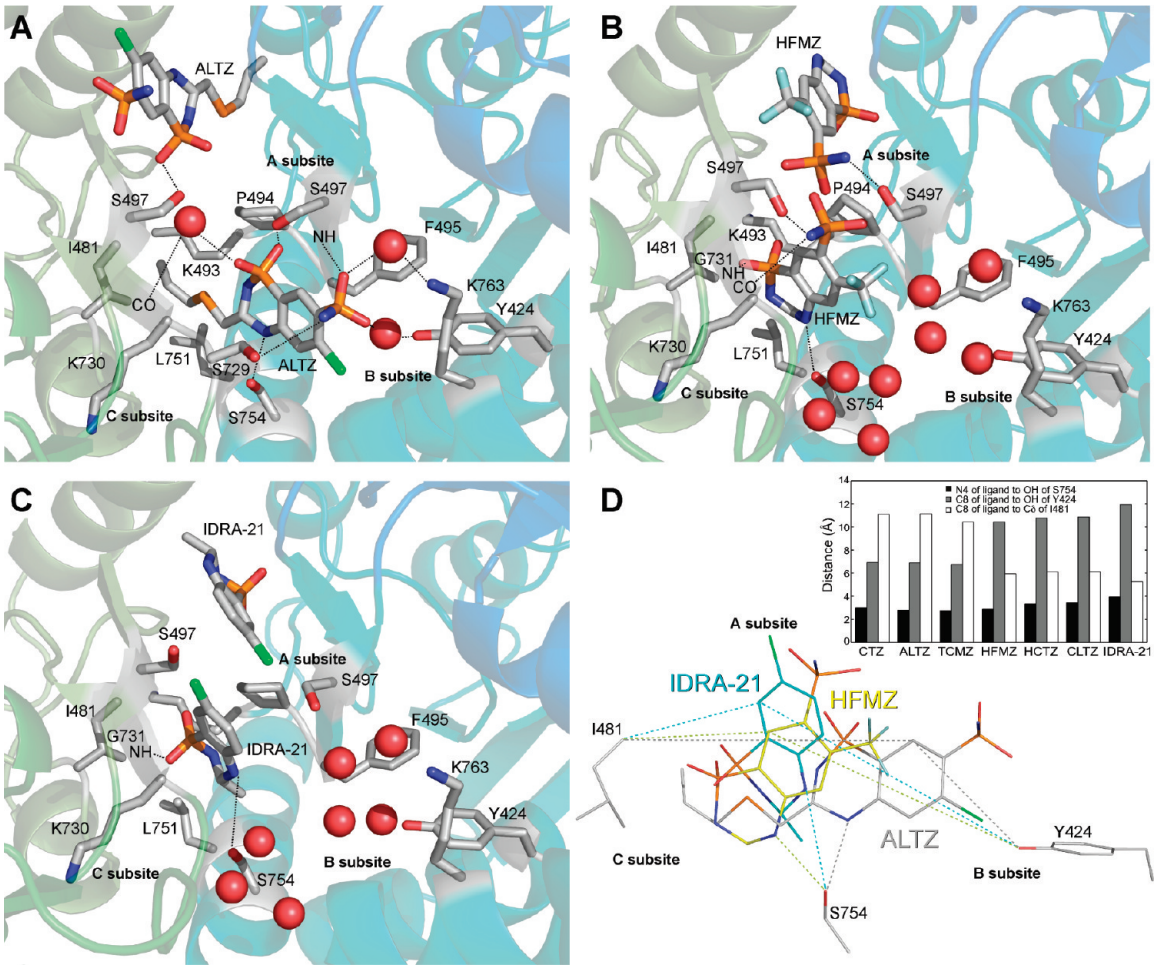

FIGURE 3: Binding of ALTZ (A), HFMZ (B), and IDRA-21 (C) to the GluR2 S1S2 dimer interface. The protein is colored as in Figure 1A. The change in bound orientation among the three compounds is shown in panel D along with a graph quantitating the movement of the rings of each of the six structures relative to the B and C subsites. Note that while only one molecule of HFMZ can bind to a dimer, two molecules are depicted to illustrate their steric incompatibility.

crevice, whereas the B subsite is more exposed and more hydrophilic. The rotation can be quantitated by measuring the distance between the C8 atom of the ligand and a residue in the B subsite (Y424) and another in the C subsite (I481). As shown in Figure 3D, the distance between the B subsite and C8 in HFMZ, HCTZ, and CLTZ increases relative to the same distance in ALTZ and TCMZ. The opposite is true for the distance to the C subsite; that is, C8 of HFMZ, HCTZ, and CLTZ moves closer to the C subsite. Perhaps the most important consequence of the shift is the change in position of the sulfonamide group. The side chain of S497 changes its rotomeric state to accommodate the position of the sulfonamide group and forms a hydrogen bond with it. The backbone carbonyl of K730 can also H-bond to the sulfonamide. This is in contrast to the hydrogen bond made by the side chain of S497 (from the other side of the dimer interface) with the sulfone of TCMZ and ALTZ. HFMZ and HCTZ form hydrophobic interactions with the side chain of P494, and the sulfone group can hydrogen bond to the backbone amide of G731. This shift moves the ring toward the center of the dimer interface [A subsite (Figure 3B)], and the position of the sulfonamide group precludes the binding of a second molecule of HFMZ, HCTZ, and CLTZ. Therefore, although two copies are found in the structure, only one can be accommodated at a given dimer interface. These results suggest that the removal of a hydrophobic group at the 3-position can lead to not only a shift in the binding site but also a change in the stoichiometry of binding.

The crystal structures suggest that because of the overlapping orientation of the two copies of HFMZ and HCTZ at the dimer interface, only one molecule would be expected to bind per dimer. HFMZ has a trifluoromethyl group, which provides an opportunity to determine the stoichiometry of binding directly. By using the high-affinity partial agonist, fluorowillardiine (FW), the agonist-binding site can be quantitatively labeled with a single fluorine. After titration with HFMZ (three fluorines per molecule), the relative extent of binding can be measured using one-dimensional ^{19}F NMR spectroscopy, with correction for the number of fluorines in HFMZ. Figure 4A shows that the binding of HFMZ saturates at approximately half the number of agonist binding sites, consistent with the crystal structure that suggests that only one copy can bind per dimer interface. The line width of the FW peak undergoes a corresponding broadening consistent with dimerization (Figure 4B).

IDRA-21. IDRA-21 is a benzothiadiazide derivative with a Cl in the 7-position (equivalent to the sulfonamide position in CTZ) and a methyl group in the 3-position. As in the other thiazides, the hydrogen bond is maintained with S754. The methyl group in the 3-position is smaller than the corresponding substituents in ALTZ, TCMZ, and CTZ, and the lack of the sulfonamide group in the 3-position eliminates a number of

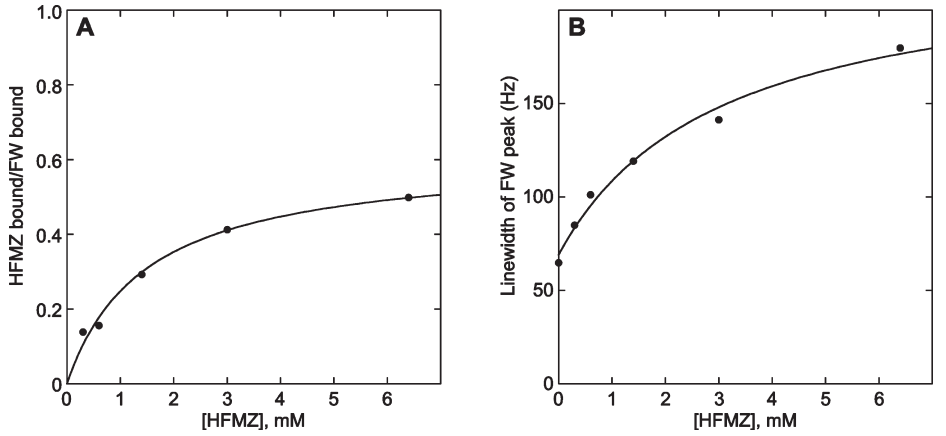

FIGURE 4: Titration of GluR2 S1S2 bound to fluorowillardiine (FW) with HFMZ. (A) Area of the bound peak for HFMZ normalized to the area of the FW-bound peak (corrected for the trifluoro group of HFMZ vs the single fluorine of FW) as a function of HFMZ concentration. The amount of bound HFMZ saturates at 60% of the bound FW. (B) Line width of the FW-bound peak as a function of HFMZ concentration. An increase in size due to dimerization would be expected to broaden the line width for bound FW. Thus, HFMZ does induce dimerization at this protein concentration (approximately 0.5 mM).

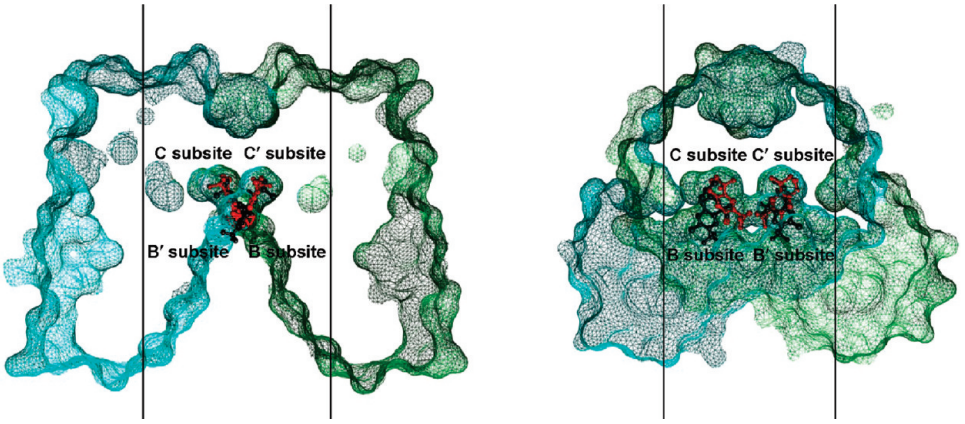

FIGURE 5: Surface cavities of GluR2 S1S2. Two viewing angles of the GluR2 S1S2 dimer reveal how TCMZ (black) and HCTZ (red) bind to the interface between subunits. HCTZ's hydrobenzothiadiazide ring shifts to a deeper position in the binding pocket. The individual subunit surfaces are colored green and cyan. For a clearer view of the inner cavity, the closest and farthest surfaces have been removed. The lines show where the surface is cut away from the neighboring view.

possible interactions in the B subsite. For these reasons, the ring rotates relative to ALTZ and TCMZ in the same plane. The methyl group in the 3-position moves into a hydrophobic C subsite lined by V750, L751, and L259 (Figure 3C). The interactions made by the sulfone remain similar to those in HFMZ, HCTZ, and CLTZ, but the ring is rotated further to an angle of approximately 60° relative to the position of ALTZ and TCMZ (Figure 3D). The Cl in the 7-position is shifted to the center of the dimer interface [A subsite (Figure 3C)], but unlike the sulfonamide from HFMZ, HCTZ, and CLTZ, the Cl atoms from both copies of IDRA-21 are accommodated within the binding site; therefore, the stoichiometry would be two per dimer interface. Diazoxide differs from IDRA-21 only by the unsaturation of the 3−4 bond. The density of diazoxide is considerably weaker than that of IDRA-21 but suggests that the orientation in the binding site changes considerably. Diazoxide resides in a position similar to that of the hydrobenzothiadiazide ring of CTZ.

DISCUSSION

Allosteric modulators bind to a large surface at the interface between two GluR2 S1S2 binding domains. In the full-length membrane-bound receptor, this would consist of two surfaces per tetrameric receptor. In the activated state, the entryway to the interface cavity is located between the membrane-bound pore and the extracellular domains. The binding surface is at the base of a large inverted U-shaped crevice between the two monomers, thereby presenting a 2-fold symmetric dimer interface (Figure 5). Crystal structures of modulator−GluR2 S1S2 complexes present a snapshot of the activated state. For modulators that act on GluR2 by retarding desensitization, a number of distinct positions can be occupied within the crevice; however, an increase in the number of interdomain linkages remains a common feature. With the creation of a more stable and favorable activated state, the energy required for the receptor to enter the desensitized state is increased leading to higher steady-state currents.

Previous structures of allosteric modulators that bind to this interface have occupied distinctly different regions of the binding surface. To understand the apparent compartmental nature of allosteric modulators, we introduced a redefinition of the binding cavity into subsites A, B, B′, C, and C′ (Figure 1B). Here, the addition of six structures to the existing modulator structures confirms the existence of distinct overlapping subsites within a larger binding surface. The previous structures of CX614 and aniracetam (*20*) specifically occupy the A subsite; however, the benzothiadiazide series illuminates the differences between the B and C subsites. The optimized binding of cyclothiazide (CTZ) to

the B and C subsites makes the modulator extremely potent; however, an inability of this molecule to cross the blood−brain barrier creates a need for designing drugs that can target AMPA receptors in vivo. The weaker affinity benzothiadiazides demonstrate which drug−receptor interactions are most important for tight binding and provide insight into the individual nature of subsites B and C.

Within the context of the symmetrical GluR2 structures, to enter the A or C subsite, the modulator must pass close to one of the B subsites. As the modulator enters the cavity, water is displaced, but only if the binding interactions are more favorable than the existing water structure. The C subsite is more hydrophobic and is buried deeper in the interface than the B subsite (Figure 5). If the molecule is only large enough to occupy either the B or C subsite (as is the case with IDRA-21, CLTZ, HFMZ, and HCTZ but not with CTZ, TCMZ, and ALTZ), then a repositioning into the C subsite is accompanied by water remaining in the exposed B subsite. The B subsite appears to have a stable arrangement of water molecules in the absence of modulator. A preference for water to enter the B subsite over the C subsite likely plays a key role in the overall energetics of benzothiadiazide binding.

The benzothiadiazide class of allosteric modulators has been extensively tested in SAR studies (*27*). On the basis of selective substitutions, Philips et al. (*27*) suggested that IDRA-21 and CTZ bind differently or to different sites on AMPA receptors. To explain the apparent SAR and functional discrepancies between CTZ and IDRA-21 derivatives, Harpsoe et al. (*26*) detailed the potential existence of alternative cavities in the GluR2 S1S2 dimer and proposed three additional cavities that are distinct from the currently known modulator-binding site. The most promising candidate is located on the opposite side of the J helix and L483 (mutation of this position to Y yields a nondesensitizing receptor) in relation to the central cavity. We were unable to observe any density that would suggest that the modulators described here are bound at that position. Clearly, from the structures presented here, IDRA-21 and CTZ bind to an overlapping site, but with a different orientation and some different interactions.

On the basis of the crystal structures of the hydrobenzothiadiazide derivatives, the differences observed in the SAR studies (*26*, *27*) can be rationalized. The high affinity of CTZ seems to be due to its optimal interaction of the norbornenyl group with the C subsite (*13*). Replacement of the 3-norbornenyl group reduces potency (*22*); however, the orientations of the bound hydrobenzothiadiazide rings remain in the B subsite for large substitutions in the 3-position [ALTZ and TCMZ (Figure 3A)]. When the substitution at the 3-position is a methyl or smaller, the hydrobenzothiadiazide rings reorient into the hydrophobic C subsite [HFMZ, HCTZ, CLTZ, and IDRA-21 (Figure 3B,C)]. The dichloromethyl in the 3-position of TCMZ is apparently large enough to prevent the reorientation of the hydrobenzothiadiazide rings; however, the contacts in the C subsite are not as extensive as for ALTZ and CTZ. Interestingly, with TCMZ bound, the subunits in the dimer are 1 Å closer than ALTZ and CTZ (as measured from the C^{α} atoms of S497), possibly suggesting that the hydrophobic void in the C subsite is drawn toward matching hydrophobic patches on the B subsite. In SAR studies, IDRA-21 has a very low tolerance for 3-position modifications larger than a methyl group (*26*).

CTZ analogues with a 5-position modification result in a loss of activity presumably due to a steric interaction with residues in the J helix (*26*). While most positions of IDRA-21 tolerate only small methyl substitutions, an alkyl substituent at the 5-position greatly enhances binding (*27*). Because of the reorientation of IDRA-21 relative to the position of CTZ, the steric hindrance that is observed for 5-position substitutions of CTZ is not present for IDRA-21 derivatives. Instead, in the crystal structure of the IDRA-21 complex, the 5-position points into the B subsite, which could easily be occupied by 5-position groups (Figure 3C).

In the cases of HFMZ, HCTZ, and CLTZ, the 7-position substituent (sulfonamide group) moves into the A subsite, and on the basis of both the electron density and the ^{19}F NMR studies, the binding of the first modulator prevents the binding of the second. That is, the change in orientation of the ring also changes the stoichiometry from two per dimer to one per dimer (Figures 3B and 4). In IDRA-21, the 7-position substitution with Cl recovers 2:1 (modulator:dimer) stoichiometry while explaining the low tolerance for larger 7-position substitutions of IDRA-21 in SAR studies (Figure 3C).

The 4-nitrogen to S754 hydrogen bond is common to all modulators studied here and separates the B and C subsites, allowing the hydrophobic modulators to pivot into the C subsite in the absence of the obstructing modification at position 3 (Figure 5). The benzothiadiazide 4-nitrogen is the major determinant of receptor desensitization kinetics (*22*). Of physiological relevance, S754 is only found in the flip form of AMPA receptors (an asparagine in the flop form) so that the hydrogen bond through the 4-nitrogen confers flip preference to the benzothiadiazide class of modulators (*25*). Clearly, a key to the understanding of the benzothiadiazide class distinction seen in SAR studies is that the B and C subsites each support a network of hydrogen bonds on opposite sides of the hydrobenzothiadiazide ring. With the exception of the 4-nitrogen to S754 tether, an intermediate orientation has no place to bind.

Measuring the increase in steady-state current, Yamada and Tang (*13*) found that CTZ was by far the most potent benzothiadiazides followed by HFMZ > HCTZ ∼ TCMZ > CLTZ. IDRA-21 and TCMZ have been studied for AMPA receptor modulation in considerably more detail than the other benzothiadiazides described here. In agonist binding experiments, IDRA-21 increases [^{3}H]AMPA and [^{3}H]FW affinity (*25*), while CTZ decreases their affinities (*24*), suggesting that interactions with different subsites within the dimer interface can produce different modulatory outcomes. The difference in binding orientations provides the hydrobenzothiadiazide ring with two unique sets of anchoring residues, which allow the rigid bridging of distinct secondary structural elements at the interface. Specific to CTZ and the other benzothiadiazides (ALTZ and TCMZ) that occupy the B subsite, hydrogen bonds link the sulfoxide to S497 and the 4-nitrogen to S754 across the B subsite and on the same side of the dimer interface (Figure 3A). Alternatively, in the IDRA-21, HFMZ, HCTZ, and CLTZ structures, the sulfoxide hydrogen bonds to the NH group of G731 across the interface (Figure 3B, C). For HFMZ, HCTZ, and CLTZ, the sulfonamide group forms a H-bond to S497, but instead of bridging the B subsite, the H-bond is made with S497 on the monomer across the interface (Figure 3B). The increased rigidity among elements lining the B subsite in CTZ, ALTZ, and TCMZ may provide clues about altered agonist binding affinities. In patch−clamp recordings of the L497Y mutant of GluR1 (equivalent to L483Y in GluR2), CTZ and TCMZ further slow desensitization but actually accelerate deactivation, whereas, CX614, which does not occupy the B subsite (*20*), further slows both desensitization and

deactivation (*34*). Since IDRA-21, HFMZ, HCTZ, and CLTZ fail to bridge S754 to elements on the same subunit much like CX614, we speculate that, in patch−clamp recordings of the same non-desensitizing mutant, deactivation in addition to desensitization should be slowed for benzothiadiazides that do not occupy the B subsite. Mitchell and Fleck (*34*) also show that the GluR1 double mutant, L497Y/S750Q (equivalent to L483Y/S754Q in GluR2), returns the L497Y mutant deactivation and EC_{50} to wild-type levels and suggest that deactivation may involve interactions specifically with residue S750 in GluR1 (S754 in GluR2). Although all of the benzothiadiazides interact with the equivalent S754, the specific orientation and therefore the bridging bonds may explain the disparity in effects on deactivation and agonist binding and may suggest a structural pathway for how modulators of the dimer interface can affect the agonist binding site. Future studies directed at highlighting the differences in desensitization and deactivation kinetics specifically for the benzothiadiazides for which we have determined structures would provide a much clearer picture of how modulator contacts are correlated with receptor function.

In summary, the binding site for allosteric modulators is a large surface at the dimer interface of the binding domain of AMPA receptors. Position 754 [either serine (flip) or asparagine (flop)] plays an important role in determining binding affinity, but the specific interactions and the orientation of hydrobenzothiadiazide in the binding site is critically dependent upon both the substituents of the ring and the saturation of the 3−4 bond. These new structures, particularly of the new hydrobenzothiadiazide binding orientation, extend our understanding of the allosteric modulator-binding site and provide useful insight for the future design of drugs.

ACKNOWLEDGMENT

We thank Prof. Gregory Weiland (Cornell University), Prof. Linda Nowak (Cornell University), Dr. Michael Fenwick (Cornell University), and Dr. Alex Maltsev (Cornell University), who provided useful discussions and important advice. JMEMolecularEditor was provided by Dr. Peter Ertl of Novartis AG.

REFERENCES

1. Dingledine, R., Borges, K., Bowie, D., and Traynelis, S. (1999) The glutamate receptor ion channels. *Pharmacol. Rev. 51*, 7–61.
2. Asztely, F., and Gustafsson, B. (1996) Ionotropic glutamate receptors. Their possible role in the expression of hippocampal synaptic plasticity. *Mol. Neurobiol. 12*, 1–11.
3. Madden, D. R. (2002) The structure and function of glutamate receptor ion channels. *Nat. Rev. Neurosci. 3*, 91–101.
4. Mayer, M. L. (2006) Glutamate receptors at atomic resolution. *Nature 440*, 456–462.
5. Oswald, R. E. (2004) Ionotropic glutamate receptor recognition and activation. *Adv. Protein Chem. 68*, 313–349.
6. Armstrong, N., and Gouaux, E. (2000) Mechanisms for activation and antagonism of an AMPA-sensitive glutamate receptor: Crystal structures of the GluR2 ligand binding core. *Neuron 28*, 165–181.
7. Mosbacher, J., Schoepfer, R., Monyer, H., Burnashev, N., Seeburg, P. H., and Ruppersberg, J. P. (1994) A molecular determinant for submillisecond desensitization in glutamate receptors. *Science 266*, 1059–1062.
8. Pei, W., Huang, Z., and Niu, L. (2007) GluR3 flip and flop: Differences in channel opening kinetics. *Biochemistry 46*, 2027–2036.
9. Black, M. D. (2005) Therapeutic potential of positive AMPA modulators and their relationship to AMPA receptor subunits. A review of preclinical data. *Psychopharmacology* (*Berlin, Ger.*) *179*, 154–163.
10. Swanson, G. T. (2009) Targeting AMPA and kainate receptors in neurological disease: Therapies on the horizon? *Neuropsychopharmacology 34*, 249–250.
11. Lee, C. R., and Benfield, P. (1994) Aniracetam. An overview of its pharmacodynamic and pharmacokinetic properties, and a review of its therapeutic potential in senile cognitive disorders. *Drugs Aging 4*, 257–273.
12. Yamada, K. A., and Rothman, S. M. (1992) Diazoxide blocks glutamate desensitization and prolongs excitatory postsynaptic currents in rat hippocampal neurons. *J. Physiol. 458*, 409–423.
13. Yamada, K. A., and Tang, C. M. (1993) Benzothiadiazides inhibit rapid glutamate receptor desensitization and enhance glutamatergic synaptic currents. *J. Neurosci. 13*, 3904–3915.
14. Arai, A., Guidotti, A., Costa, E., and Lynch, G. (1996) Effect of the AMPA receptor modulator IDRA 21 on LTP in hippocampal slices. *NeuroReport 7*, 2211–2215.
15. Thompson, D. M., Guidotti, A., DiBella, M., and Costa, E. (1995) 7-Chloro-3-methyl-3,4-dihydro-2H-1,2,4-benzothiadiazine S,S-dioxide (IDRA 21), a congener of aniracetam, potently abates pharmacologically induced cognitive impairments in patas monkeys. *Proc. Natl. Acad. Sci. U.S.A. 92*, 7667–7671.
16. Zivkovic, I., Thompson, D. M., Bertolino, M., Uzunov, D., DiBella, M., Costa, E., and Guidotti, A. (1995) 7-Chloro-3-methyl-3,4-dihydro-2H-1,2,4-benzothiadiazine S,S-dioxide (IDRA 21): A benzothiadiazine derivative that enhances cognition by attenuating DL-α-amino-2,3-dihydro-5-methyl-3-oxo-4-isoxazolepropanoic acid (AMPA) receptor desensitization. *J. Pharmacol. Exp. Ther. 272*, 300–309.
17. Stern-Bach, Y., Russo, S., Neuman, M., and Rosenmund, C. (1998) A point mutation in the glutamate binding site blocks desensitization of AMPA receptors. *Neuron 21*, 907–918.
18. Sun, Y., Olson, R., Horning, M., Armstrong, N., Mayer, M., and Gouaux, E. (2002) Mechanism of glutamate receptor desensitization. *Nature 417*, 245–253.
19. Partin, K. M., Fleck, M. W., and Mayer, M. L. (1996) AMPA receptor flip/flop mutants affecting deactivation, desensitization, and modulation by cyclothiazide, aniracetam, and thiocyanate. *J. Neurosci. 16*, 6634–6647.
20. Jin, R., Clark, S., Weeks, A. M., Dudman, J. T., Gouaux, E., and Partin, K. M. (2005) Mechanism of positive allosteric modulators acting on AMPA receptors. *J. Neurosci. 25*, 9027–9036.
21. Kaae, B. H., Harpsoe, K., Kastrup, J. S., Sanz, A. C., Pickering, D. S., Metzler, B., Clausen, R. P., Gajhede, M., Sauerberg, P., Liljefors, T., and Madsen, U. (2007) Structural proof of a dimeric positive modulator bridging two identical AMPA receptor-binding sites. *Chem. Biol. 14*, 1294–1303.
22. Hald, H., Ahring, P. K., Timmermann, D. B., Liljefors, T., Gajhede, M., and Kastrup, J. S. (2009) Distinct Structural Features of Cyclothiazide are Responsible for Effects on Peak Current Amplitude and Desensitization Kinetics at iGluR2. *J. Mol. Biol.* DOI: 10.1016/j.jmb.2009.1007.1002.
23. Arai, A. C., Kessler, M., Rogers, G., and Lynch, G. (2000) Effects of the potent ampakine CX614 on hippocampal and recombinant AMPA receptors: Interactions with cyclothiazide and GYKI 52466. *Mol. Pharmacol. 58*, 802–813.
24. Kessler, M., and Arai, A. C. (2006) Use of [^{3}H]fluorowillardiine to study properties of AMPA receptor allosteric modulators. *Brain Res. 1076*, 25–41.
25. Arai, A. C., Xia, Y. F., Kessler, M., Phillips, D., Chamberlin, R., Granger, R., and Lynch, G. (2002) Effects of 5′-alkyl-benzothiadiazides on (R,S)-α-amino-3-hydroxy-5-methyl-4-isoxazolepropionic acid (AMPA) receptor biophysics and synaptic responses. *Mol. Pharmacol. 62*, 566–577.
26. Harpsoe, K., Varming, T., Gouliaev, A. H., Peters, D., and Liljefors, T. (2007) Identification of a putative binding site for 5-alkyl-benzothiadiazides in the AMPA receptor dimer interface. *J. Mol. Graphics Modell. 26*, 213–225.
27. Phillips, D., Sonnenberg, J., Arai, A. C., Vaswani, R., Krutzik, P. O., Kleisli, T., Kessler, M., Granger, R., Lynch, G., and Richard Chamberlin, A. (2002) 5′-Alkyl-benzothiadiazides: A new subgroup of AMPA receptor modulators with improved affinity. *Bioorg. Med. Chem. 10*, 1229–1248.
28. Hollmann, M., and Heinemann, S. (1994) Cloned glutamate receptors. *Annu. Rev. Neurosci. 17*, 31–108.
29. Otwinowski, Z., and Minor, W. (1997) Processing of X-ray diffraction data collected in oscillation mode. In Methods in Enzymology (Carter, C. W., and Sweet, R. M., Eds.) Vol. 276, pp 307−326, Macromolecular Crystallography, Part A, Academic Press, New York.
30. Adams, P. D., Grosse-Kunstleve, R. W., Hung, L. W., Ioerger, T. R., McCoy, A. J., Moriarty, N. W., Read, R. J., Sacchettini, J. C., Sauter, N. K., and Terwilliger, T. C. (2002) PHENIX: Building new software for automated crystallographic structure determination. *Acta Crystallogr. D58*, 1948–1954.

31. Emsley, P., and Cowtan, K. (2004) Coot: Model-building tools for molecular graphics. *Acta Crystallogr. D60*, 2126–2132.
32. Delaglio, F., Grzesiek, S., Vuister, G. W., Zhu, G., Pfeifer, J., and Bax, A. (1995) NMRPipe: A multidimensional spectral processing system based on UNIX pipes. *J. Biomol. NMR 6*, 277–293.
33. Ahmed, A. H., Wang, Q., Sondermann, H., and Oswald, R. E. (2008) Structure of the S1S2 glutamate binding domain of GluR3. *Proteins: Struct., Funct., Bioinf. 75*, 628–637.
34. Mitchell, N. A., and Fleck, M. W. (2007) Targeting AMPA receptor gating processes with allosteric modulators and mutations. *Biophys. J. 92*, 2392–2402.